ISSN 1063-7710, Acoustical Physics, 2018, Vol. 64, No. 5, pp. 596–604. © Pleiades Publishing, Ltd., 2018.

ACOUSTIC SIGNAL PROCESSING AND COMPUTER SIMULATION

A Mixed Analytical-Numerical Method for the Vibro-Acoustic Analysis of an Underwater Ring-Stiffened Cylindrical Shell Containing Substructures[1]

Ming-Song Zou[a, b, *], You-Sheng Wu[a, b], Jian-De Liu[a], and Shu-Xiao Liu[a]

[a] *China Ship Scientific Research Center, Wuxi 214082, China*

[b] *National Key Laboratory on Ship Vibration and Noise, Wuxi 214082, China*

**e-mail: zoumings@126.com*

Received October 20, 2017

Abstract— A new sono-elastic substructure method is proposed in this paper to improve the computational efficiency of the hull-substructure coupled and fluid-structure interacted vibration and acoustic radiation of a submerged cylindrical-shell-type vehicle. The typical part of the vehicle structure is divided into the main hull and the internal substructures. The fluid-structure interaction problem of the main hull is solved by an analytical method based on the simplified model of a single-hull ring-stiffened cylindrical shell simply supported at both ends. Meanwhile, the substructures are numerically modeled through the Finite Element Method, with the condensed dynamic stiffness matrices of them obtained via the Superelement Method of Modal Synthesis. The main hull and the internal substructures are then integrated according to the boundary compatibility conditions at the connecting parts. Thus, a Mixed Analytical-Numerical Substructure (MANS) method is formulated. The applicability of this method is validated by two numerical examples as well as the test results of a large-scale submerged structural model. It is shown that the MANS method is suitable for the prediction of vibration and acoustic radiation of typical cylindrical-shell-type submerged structures in the medium frequency region.

Keywords: hydroelasticity, sono-elasticity, dynamic substructure method, cylindrical shell, acoustic radiation

DOI: 10.1134/S1063771018050111

1. INTRODUCTION

Since the 1980s great progress has been made in the field of dynamic substructure methods, which synthesize the calculated or measured dynamic characteristics of all decomposed substructures to obtain the dynamic behaviors of the entire structure [1, 2]. This kind of method was applied in the analysis of fluid-structure interactions and dynamic responses of structures [1, 3, 4]. Persson et al. [5] analyzed the vibration characteristics of a complex water-pipe system using the component mode synthesis method, which is similar to the dynamic substructure method. The dynamic substructure method is also used to obtain the elastic response of submerged shells with internally attached structures to shock loading [6]. In the work of Soize [7], in order to predict the vibrations and acoustic radiations of a complex structure, the structural system was divided into a main structure that was interacting with surrounding fluid, and several substructures with uncertain stiffness and mass distributions, which were then represented as the structures of fuzzy characteristics by using probabilistic method. Franzoni and Park [8], Park [9] proposed a method where the dynamic characteristics of the low-resolution main structure and the high-resolution substructures were independently solved and integrated by employing finite element models with different mesh sizes or analytical models. In the vibration analysis of the main structure [10], the structure system was decomposed to the main structure and the subordinate substructures. The latter together with their conjunction boundaries were simplified to some extent. In the work of Pratellesi et al. [11], a hybrid formulation was derived for medium frequency analysis of assembled structures made of two subsystems, the low frequency part is modelled with finite element, whereas the flexible part is modelled with the Smooth Integral Formulation (SIF). In the works of Meyer et al. [12, 13], the Condensed Transfer Function (CTF) method was proposed to predict the vibro-acoustic behavior of a submerged shell with non-axisymmetric internal substructures. Based on the technology of supercell

[1] The article is published in the original.

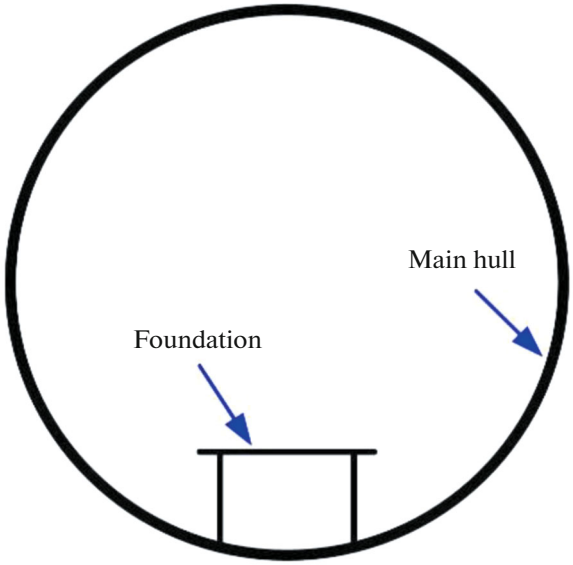

Fig. 1. Schematic diagram of a cylindrical ship hull.

modelling and analytical modelling, Salin et al. [14] proposed a method which allows to carry out analysis in the expanded frequency range for finite-element models of any complexity. Suvorov et al. [15] introduced a method for nonconformal finite-element simulation of the region of interaction between an acoustic fluid and deformed solid bodies, where special contact finite elements are used.

The method described in this paper contains both the common characteristics of dynamic substructure methods and the characteristics of the hydroelastic analysis in acoustic medium.

In vibration and noise control of a ship, modification or optimization of some substructure design (such as a machinery foundation etc.) is usually required. In redesigning a substructure, if the main structure is assumed to be a prescribed simplified boundary condition of the substructure and the interaction between them is neglected, the predicted dynamic behavior of the local optimization may not reach the expected target of vibration and noise reduction due to the actual influence of the main hull.

If the main hull and substructure are assembled to establish a fluid-structure interaction model for the vibration and noise predictions, any slight modification in one of the substructures will lead to recalculation of the entire model with greatly increased computational effort. To reduce the demand on computational resources, an approach called the Sono-elastic Substructure Separation and Integration (SSSI) Method was proposed [16, 17]. To achieve the same purpose, a Mixed Analytical-Numerical Substructure (MANS) method is proposed in this paper to solve

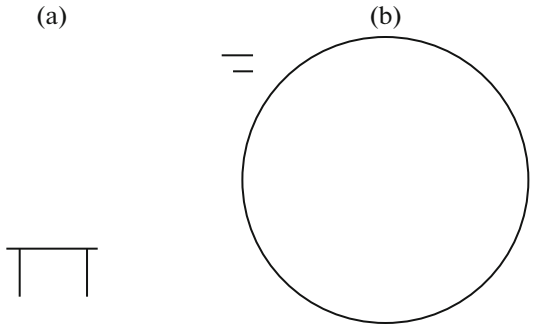

Fig. 2. Segmentation of the ship structure: (a) foundation; (b) main hull.

acoustic radiation problems of an underwater cylindrical hull structure in medium frequency region from the loop frequency to about 700 Hz. The loop frequency of a cylindrical shell is defined such that the length of longitudinal wave at this frequency is equal to the circumference of the hull. In this medium frequency region, the vibration modes of a cylindrical hull are very intensive. To calculate all the modes in this frequency region by Finite Element Method (FEM) requires great computational time and usually gives uncertain precision. For this regard, the Statistical Energy Analysis method (SEA) may be adopted instead of FEM to describe the vibration characteristics of the ship hull. However, the calculation error of SEA method will also be large because the scale of substructures in a ship is usually small comparing with the main hull of the ship, and the modal density of the global structure is not high enough. To improve the prediction accuracy, in the present MANS method the analytical model is used for the main hull, and the finite element model is adopted for the substructures to predict the sono-elastic responses of the underwater structure, including the acoustic radiations. Numerical examples are given in this paper to compare the predictions by the present MANS method and those by the three-dimensional sono-elastic analysis method [18] and the SEA method. The predictions are also compared with the results of a model test. It is shown that this mixed structural model may well fit the needs of predicting the acoustic radiation problem in the medium frequency region.

2. THE SONO-ELASTIC SUBSTRUCTURE METHOD OF A SUBMERGED STRUCTURE

Figure 1 shows a typical underwater cylindrical ship hull which consists of the main hull and the machinery foundation. The structure can be divided into two parts to illustrate the sono-elastic substructure method as shown in Fig. 2.

The vibration equations of the fluid-structure interaction system of the main hull are [17, 19]:

$$\left(-\omega^2[M_A]+i\omega[C_A]+[K_A]\right)\{q\}=[D_A]^{\mathrm{T}}\begin{pmatrix}\{F_{A1}\}\\ \{F_{A2}\}\end{pmatrix}, \quad (1)$$

where $\{q\}$ are the principal coordinates of the main hull, ω is the angular frequency, $[M_A]$, $[K_A]$ and $[C_A]$ are respectively matrices of the generalized structural mass combined with the generalized fluid added mass, the generalized structural stiffness combined with the fluid restoring force coefficients, and the generalized structural damping combined with the fluid radiation damping coefficients. $\{F_{A1}\}$ is the column vector of exciting force acting on the main hull, $\{F_{A2}\}$ is the column vector of the connection force acting on the boundary of the main hull and the substructure, $[D_A]$ is matrix of principal modes at the positions of the exciting forces and connecting forces. The superscript "T" denotes the matrix transposition.

According to Eq. (1), a generalized dynamic stiffness matrix of the main hull can be derived as

$$[S_A]=-\omega^2[M_A]+i\omega[C_A]+[K_A]. \quad (2)$$

By introducing a set of virtual modes of the main hull, and the corresponding generalized coordinates $\{q_{\mathrm{vi}}\}$, the dynamic equations of motion of the main hull may be expressed as

$$\begin{pmatrix}[S_A] & [0]\\ [0] & [S_{\mathrm{vi}}]\end{pmatrix}\begin{pmatrix}\{q\}\\ \{q_{\mathrm{vi}}\}\end{pmatrix}=\begin{pmatrix}[D_A]^{\mathrm{T}}\\ [I]\end{pmatrix}\begin{pmatrix}\{F_{A1}\}\\ \{F_{A2}\}\end{pmatrix}, \quad (3)$$

where [0] is a zero matrix, $[I]$ is a unit diagonal matrix. If $[S_{\mathrm{vi}}]$ is also a unit diagonal matrix, Eq. (3) reduces to

$$\{q_{\mathrm{vi}}\}=\begin{pmatrix}\{F_{A1}\}\\ \{F_{A2}\}\end{pmatrix}. \quad (4)$$

Substituting Eq. (4) into Eq. (3), the following equation may be obtained:

$$\{q\}=[S_A]^{-1}[D_A]^{\mathrm{T}}\{q_{\mathrm{vi}}\}. \quad (5)$$

The dynamic displacement $\{\xi_{A1}\}$ at the positions of the exciting forces on the main hull, and the displacement $\{\xi_{A2}\}$ at the connection points between the main hull and the substructure can be written as:

$$\begin{pmatrix}\{\xi_{A1}\}\\ \{\xi_{A2}\}\end{pmatrix}=[D_A]\{q\}=\begin{pmatrix}[D_{A1}]\\ [D_{A2}]\end{pmatrix}\{q\}. \quad (6)$$

After the finite element model of the substructure is established, the input and output dynamic stiffness matrices of the substructure may be generated by the Super-element Method of Modal Synthesis (SMMS) [20]. The vibration equations of the substructure may then be written in the form:

$$[Z_B]\begin{pmatrix}\{\eta_{B1}\}\\ \{\eta_{B2}\}\end{pmatrix}=\begin{pmatrix}\{F_{B1}\}\\ \{F_{B2}\}\end{pmatrix}, \quad [Z_B]=\begin{pmatrix}[Z_{B11}] & [Z_{B12}]\\ [Z_{B21}] & [Z_{B22}]\end{pmatrix}, \quad (7)$$

where $[Z_B]$ is the condensation dynamic stiffness matrix of the substructure, $\{\eta_{B1}\}$ and $\{F_{B1}\}$ are respectively the displacements and forces at the position of the external excitation on the substructure, $\{\eta_{B2}\}$ and $\{F_{B2}\}$ are respectively the displacements and forces at the connection points between main hull and substructure.

The displacements and the internal forces in the connection of the main hull and the substructure should satisfy the conditions of continuity:

$$\{\xi_{A2}\}=\{\eta_{B2}\}, \quad (8a)$$

$$\{F_{A2}\}=-\{F_{B2}\}. \quad (8b)$$

Let $[I]=\begin{pmatrix}[I_1]\\ [I_2]\end{pmatrix}$, $[C_2]=[D_{A2}][S_A]^{-1}[D_A]^{\mathrm{T}}$. In combination with the continuity conditions, the coupled dynamic equations are obtained [17]:

$$\begin{pmatrix}[Z_{B11}] & [Z_{B12}][C_2]\\ [Z_{B21}] & [Z_{B22}][C_2]+[I_2]\\ [0] & [I_1]\end{pmatrix}\begin{pmatrix}\{\eta_{B1}\}\\ \{q_{\mathrm{vi}}\}\end{pmatrix}=\begin{pmatrix}\{F_{B1}\}\\ \{0\}\\ \{F_{A1}\}\end{pmatrix}. \quad (9)$$

The solutions provide the displacements $\{\eta_{B1}\}$ at the position of the external excitation on the substructure and the virtual modal generalized coordinates $\{q_{\mathrm{vi}}\}$ of the main hull. The principal coordinates of the main hull $\{q\}$ may then be obtained by Eq. (5).

3. THE MIXED ANALYTICAL-NUMERICAL SUBSTRUCTURE (MANS) METHOD

The main hull model can be treated as a single cylindrical shell with equally spaced ring stiffeners, two simply supported ends, each attached, but not connected with, an infinitely long rigid pillar of the same diameter as acoustic barriers as shown in Fig. 3. The model is submerged in an ideal unbounded acoustic fluid field. Both rigid pillars provide the artificial fixed rigid acoustic boundary conditions for analytic solution. The origin of the rectangular coordinate system *xyz* is located at the center of the cylindrical shell. There exists an analytical solution to the vibratory response and acoustic radiation of this ring-stiffened cylindrical shell [21].

Omitting the harmonic time factor $e^{i\omega t}$ in the frequency domain, the vibration displacement of the

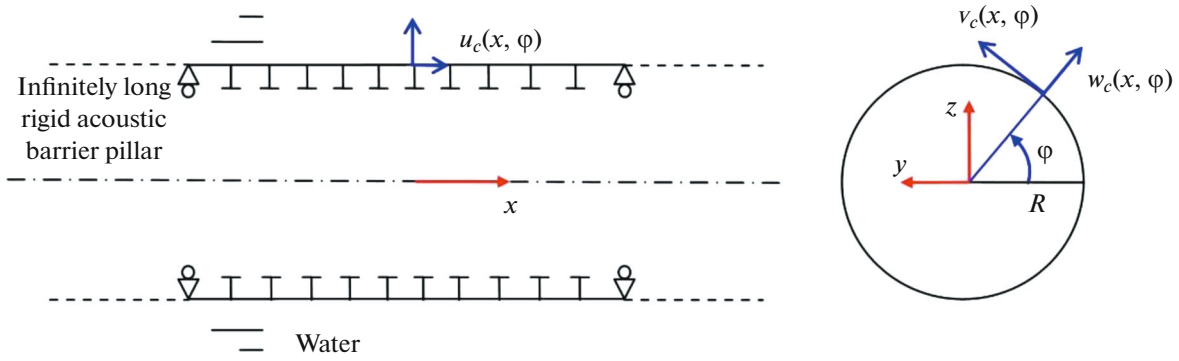

Fig. 3. Analytical calculation model of a single ring-stiffened cylindrical shell.

ring- stiffened cylindrical shell acted by a sinusoidal exciting force of the frequency ω can be written as [22]

$$\begin{cases} u_c(x,\varphi) = \left[\sum_{m=0}^{\infty}\sum_{n=0}^{\infty}\bar{U}_{mn}\cos n\varphi\ \cos\left(\frac{m\pi x}{L}+\frac{m\pi}{2}\right)\right] \\ + \left[\sum_{m=0}^{\infty}\sum_{n=0}^{\infty}\tilde{U}_{mn}\sin n\varphi\cos\left(\frac{m\pi x}{L}+\frac{m\pi}{2}\right)\right], \\ v_c(x,\varphi) = \left[\sum_{m=0}^{\infty}\sum_{n=0}^{\infty}\bar{V}_{mn}\sin n\varphi\ \sin\left(\frac{m\pi x}{L}+\frac{m\pi}{2}\right)\right] \\ + \left[\sum_{m=0}^{\infty}\sum_{n=0}^{\infty}\tilde{V}_{mn}\cos n\varphi\sin\left(\frac{m\pi x}{L}+\frac{m\pi}{2}\right)\right], \\ w_c(x,\varphi) = \left[\sum_{m=0}^{\infty}\sum_{n=0}^{\infty}\bar{W}_{mn}\cos n\varphi\ \sin\left(\frac{m\pi x}{L}+\frac{m\pi}{2}\right)\right] \\ + \left[\sum_{m=0}^{\infty}\sum_{n=0}^{\infty}\tilde{W}_{mn}\sin n\varphi\sin\left(\frac{m\pi x}{L}+\frac{m\pi}{2}\right)\right], \end{cases} \quad (10)$$

where the subscript "m" is the axial half-wave number, the subscript "n" is the circumferential wave number, $u_c(x,\varphi)$, $v_c(x,\varphi)$ and $w_c(x,\varphi)$ are respectively the axial, tangential and normal displacement at the position (x,φ) of the cylindrical shell. L is the length of the cylindrical shell. $\bar{U}_{mn}$, $\bar{V}_{mn}$, $\bar{W}_{mn}$, $\tilde{U}_{mn}$, $\tilde{V}_{mn}$ and $\tilde{W}_{mn}$ are generalized coordinates respectively.

In general, the modal superposition of the complete set orthogonal modes in Eq. (10) may be truncated to $m = M$ and $n = N$. M and N may be determined by trial calculation for convergence in the required frequency region. In the case where the substructure is coupled with the main hull, the truncated mode order in the azimuth direction N (truncated circumferential mode order) and the truncated mode order in the longitudinal direction M (truncated axial mode order) should be sufficiently large to guarantee the precision of this method. The generalized coordinates of the main hull may then be expressed as a column vector

$$\{q\} = \left(\{q_0\}^{\mathrm{T}}, \{q_1\}^{\mathrm{T}}, \cdots, \{q_N\}^{\mathrm{T}}\right)^{\mathrm{T}}, \quad (11)$$

where $\{q_n\}$ denotes the generalized coordinates for circumferential wave number n:

$$\{q_n\} = \{\bar{W}_{0n}, \cdots, \bar{W}_{Mn}, \tilde{W}_{0n}, \cdots, \tilde{W}_{Mn}, \bar{V}_{0n}, \cdots, \bar{V}_{Mn}, \tilde{V}_{0n}, \cdots, \tilde{V}_{Mn}, \bar{U}_{0n}, \cdots, \bar{U}_{Mn}, \tilde{U}_{0n}, \cdots, \tilde{U}_{Mn}\}^{\mathrm{T}}. \quad (12)$$

When the structural damping effect of the main hull is represented by the complex Young's modulus and the hydrodynamic coefficients are also expressed as the complex form to include the generalized added mass and the generalized hydrodynamic damping, the fluid-structure interaction equations can be expressed in the form [17]

$$\left(-\omega^2[M_{sn}] + [K_{sn}]\right)\{q_n\} = [S_{An}]\{q_n\} = \{F_n\}, \quad (13)$$

where $\{F_n\}$ is the generalized exciting force, and $[S_{An}]$ is the generalized dynamic stiffness matrix of the main hull for circumferential wave number n. The expressions of the elements in the matrices of Eq. (13) can be found in [17].

Because the single ring-stiffened cylindrical shell is an axisymmetric structure, the modals of the main hull with different circumferential wave numbers are decoupled. The entire generalized dynamic stiffness matrix of the main hull may then be expressed as a block diagonal matrix:

$$[S_A] = \begin{pmatrix} [S_{A0}] & \cdots & [0] & \cdots & [0] \\ \vdots & \ddots & \vdots & \iddots & \vdots \\ [0] & \cdots & [S_{An}] & \cdots & [0] \\ \vdots & \iddots & \vdots & \ddots & \vdots \\ [0] & \cdots & [0] & \cdots & [S_{AN}] \end{pmatrix}. \quad (14)$$

In assembling the main hull (the stiffened cylindrical shell) and the substructure (the foundation, for example), a consistent coordinate system should be

used. After conversion of the physical quantities of the substructure in its rectangular coordinate system into the cylindrical coordinate system of the stiffened cylindrical shell, the mixed analytical-numerical coupled equations of motion between the main hull and substructures can be written as

$$\begin{pmatrix} [Z_{B\mathrm{cy}11}] & [Z_{B\mathrm{cy}12}][C_2] \\ [Z_{B\mathrm{cy}21}] & [Z_{B\mathrm{cy}22}][C_2]+[I_2] \\ [0] & [I_1] \end{pmatrix} \begin{pmatrix} \{\eta_{B\mathrm{cy}1}\} \\ \{q_{\mathrm{vi}}\} \end{pmatrix} = \begin{pmatrix} \{F_{B\mathrm{cy}1}\} \\ \{0\} \\ \{F_{A1}\} \end{pmatrix}, \quad (15)$$

where the subscript "*B*cy" denotes the quantity of the substructure described in the cylindrical coordinate system. When implementing a coupled analysis of the main hull and the substructure, the computation speed is mainly determined by Eq. (15). The dimension of the matrix in Eq. (15) is approximately equal to the connecting degree of freedom (DOF) between the main hull and the substructure. As the connecting DOF increases, the time cost of computation also rises.

In calculation of $[C_2] = [D_{A2}][S_A]^{-1}[D_A]^{\mathrm{T}}$, the generalized dynamic stiffness matrix of the main hull contains the generalized hydrodynamic coefficients of the stiffened cylindrical shell. They may be calculated analytically in the form of a complex function [17, 23]

$$G_{\alpha\beta n} = \varepsilon_n \pi R \times \int_{-L/2}^{L/2} \left\{ \frac{1}{2\pi} \int_{-\infty}^{\infty} \frac{\tilde{Z}_n(k_x)}{i\omega} \left[\int_{-L/2}^{L/2} \sin\left(\frac{\alpha\pi x}{L} + \frac{\alpha\pi}{2}\right) e^{ik_x x} dx \right] \times e^{-ik_x x} dk_x \right\} \sin\left(\frac{\beta\pi x}{L} + \frac{\beta\pi}{2}\right) dx, \quad (16)$$

where the real part is the generalized added mass and the imaginary part is the radiation damping coefficient. While $\varepsilon_n = \begin{cases} 2 & n = 0 \\ 1 & n > 0 \end{cases}$, $\tilde{Z}_n(k) = -i\omega\rho_0 R \left[n - \sqrt{k^2 - k_x^2} R \frac{H_{n+1}^{(2)}(\sqrt{k^2 - k_x^2} R)}{H_n^{(2)}(\sqrt{k^2 - k_x^2} R)} \right]^{-1}$, R is the radius of the cylindrical shell, $H_n^{(2)}(\,)$ is the n^{th} order second Hankel function respectively, ρ_0 is the water density, k is the acoustic wave number in water. If $k^2 < k_x^2$, then $\sqrt{k^2 - k_x^2} = -i\sqrt{k_x^2 - k^2}$.

The calculation of generalized hydrodynamic coefficients shown in Eq. (16) have been studied by several researchers. The conventional method is calculating the coefficients through straightforward numerical integration (for example, see [23]). In this paper, a more efficient method is adopted. The fast Fourier transform (FFT) algorithm is used to calculate integrals $\left\{ \frac{1}{2\pi} \int_{-\infty}^{\infty} \frac{\tilde{Z}_n(k_x)}{i\omega} \left[\int_{-L/2}^{L/2} \sin\left(\frac{\alpha\pi x}{L} + \frac{\alpha\pi}{2}\right) e^{ik_x x} dx \right] e^{-ik_x x} dk_x \right\}$ [24]. The calculation speed can be effectively improved in this way. Calculating generalized hydrodynamic coefficients using the FFT is also much faster than the numerical boundary element method (BEM). In the process of calculation, the generalized hydrodynamic coefficients of the cylindrical shell are computed beforehand and saved in a data file, which can be read in the subsequent analytical–numerical coupled calculation. As long as the parameters of the cylindrical shell remain the same, the generalized hydrodynamic coefficients data can be re-read and used repeatedly, which will greatly improve the computational efficiency.

Once the virtual generalized coordinates $\{q_{\mathrm{vi}}\}$ are solved by Eq. (15), the generalized coordinates of the main hull $\{q\}$ may be obtained, the vibration responses and the radiated sound power in water can be solved further [17, 18]. The radiated sound power of the up–down symmetric modes $\bar{P}_n(\omega)$ and antisymmetric modes $\tilde{P}_n(\omega)$ corresponding to each circumferential wave number n can be written as

$$\bar{P}_n(\omega) = \frac{1}{2} \mathrm{Re} \left\{ \sum_{\beta=1}^{M} \sum_{\alpha=1}^{M} \left[(i\omega)^2 \bar{W}_{\alpha n} G_{\alpha\beta n} (i\omega \bar{W}_{\beta n})^* \right] \right\}, \quad (17a)$$

$$\tilde{P}_n(\omega) = \frac{1}{2} \mathrm{Re} \left\{ \sum_{\beta=1}^{M} \sum_{\alpha=1}^{M} \left[(i\omega)^2 \tilde{W}_{\alpha n} G_{\alpha\beta n} (i\omega \tilde{W}_{\beta n})^* \right] \right\}, \quad (17b)$$

where the superscript "*" is the conjugation symbol.

The total radiated sound power and the sound source level can be written as

$$P_{all}(\omega) = \sum_{n=0}^{N} \bar{P}_n(\omega) + \sum_{n=1}^{N} \tilde{P}_n(\omega), \quad (18)$$

$$L_p(\omega) = 10 \log \frac{P_{all}(\omega)/(4\pi)}{0.67 \times 10^{-18}}. \quad (19)$$

4. NUMERICAL EXAMPLES

The model shown in Fig. 4 is adopted as the first example for validation of the MANS method. The dimensions of the model are shown in the Table 1. The density, Young's modulus, Poisson's ratio and damping ratio of the shell and foundation material are the same—7800 kg/m^3, 2.1 × 10^{11} N/m^2, 0.3 and 0.01 respectively. The cylindrical shell is simply supported at both ends. The rigid pillars at both ends used as the acoustic barriers have the length five times as the shell length. The foundation is fixed at the elastic cylindrical shell. The structural model is submerged in an unbounded water domain.

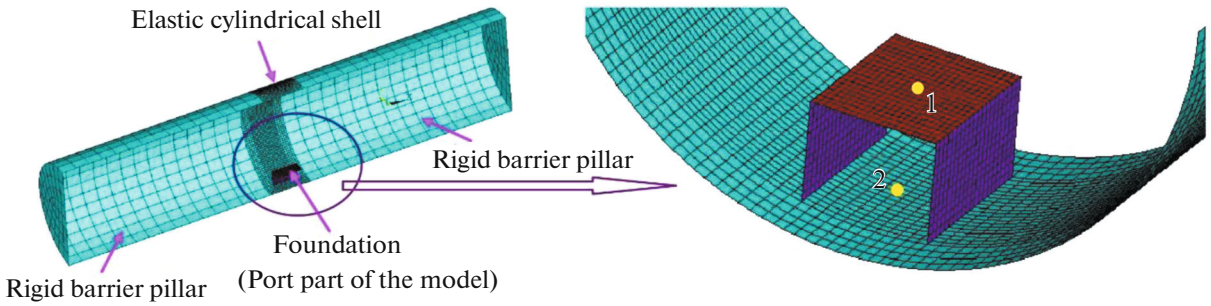

Fig. 4. The calculation model for validating the MANS method.

The variations of structural velocity and radiated sound power in water with regard to frequencies induced by excitations of sinusoidal forces with unit amplitude acting vertically at the Position 1 and Position 2 as shown in Fig. 4 are calculated in this section by two methods for comparison. The first is the present MANS method (marked as "Mixed analytical–numerical results" in comparisons), and the second is the three-dimensional sono-elastic analysis method [17, 18] (marked as "Numerical results" in comparisons). The latter is the extension of the previous three-dimensional hydroelasticity theory of ships [19] to allow for the effect of fluid compressibility being included by employing the Green's function of the Pekeris ocean hydro-acoustic waveguide model [25, 26], and hence to enable the sono-elastic responses and the acoustic radiations of a ship excited by onboard machineries being predicted in the ocean hydro-acoustic environment. The truncated axial and circumferential mode orders used in the MANS method are $M = 30$ and $N = 25$.

The Position 1 is on the foundation panel and the Position 2 is on the cylindrical shell right below Position 1. Figure 5 shows that under the excitation of a vertical unit force at the Position 1, the results predicted by the two methods of the velocity responses and the source level of the radiated sound power agree with each other quite well. This in a way validates the correctness of the MANS method. The small differences in the frequency region above 150 Hz in Fig. 5b, 5c are mainly due to the fact that the numerical sono-elastic analysis method cannot simulate the infinite long rigid pillar used in MANS method.

The main hull in this work is described using the analytical model of an equidistantly ribbed cylindrical shell. The ribs are of the same scantlings and distributed equidistantly along the longitudinal axis of the cylinder. The radius and thickness of the cylindrical shell, the scantling of the ribs, and the length of spans between two adjacent ribs are all variable parameters. The substructures are addressed using finite element models and can be any complex structure. In the engineering practice, the main hull is not usually the ideal model, i.e., the equidistantly ribbed cylindrical shell. For example, the model shown in Fig. 6 is not of an ideal axisymmetric shape. Under most circumstances, the models that have small derivations can be addressed approximately to the equidistantly ribbed cylindrical shell model without losing a satisfactory precision.

The second example is a ring-stiffened cylindrical shell structure of the radius 2.5 m with the foundation type substructure as shown in Fig. 6. The underwater acoustic radiation caused by a unit vertical force acting on the foundation is calculated by the MANS method, the numerical sono-elastic analysis method [17, 18] and the SEA method in unbounded water domain. In the calculation the frequency range covers the low, medium and high frequency regions. The numerical sono-elastic analysis method is applicable in the low frequency region, usually below several hundred Hz. The results of SEA method are calculated by using the AutoSEA software, and is usually valid in the high frequency region. The truncated axial and circumferential mode orders used in the MANS method are $M = 44$ and $N = 22$. Figure 7 shows that the MANS method is suitable for prediction of the acoustic radiation of

Table 1. Parameters of the model

Cylindrical shell			Foundation				
Radius	Length	Thickness	Length	Width	Height	Panel thickness	Web thickness
2.65 m	2 m	26 mm	1.2 m	1 m	0.8 m	30 mm	20 mm

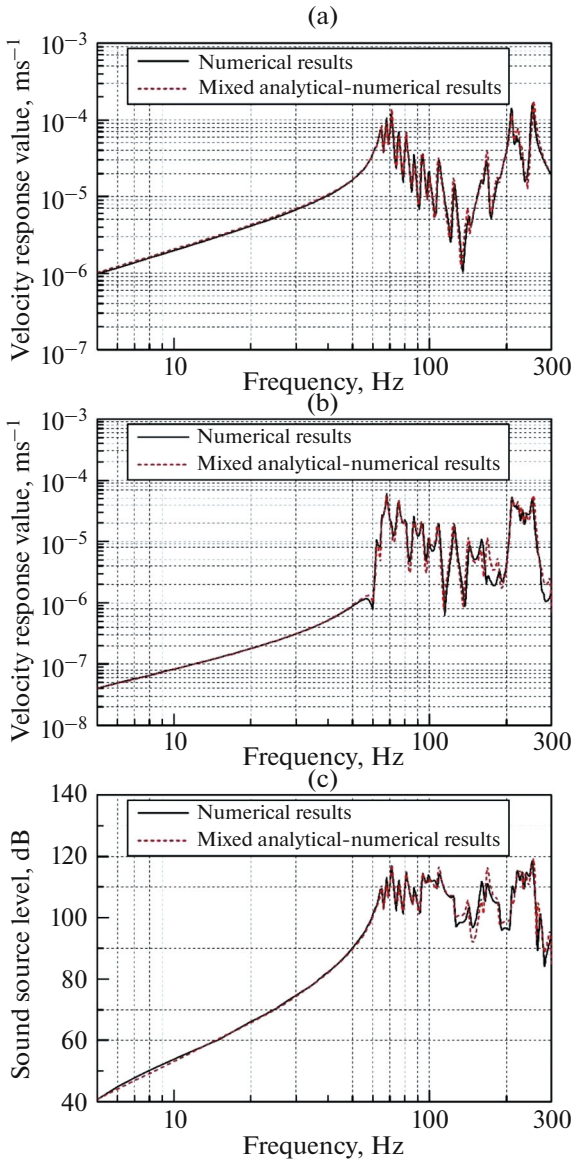

Fig. 5. Comparison of structural vibration and underwater acoustic radiation of the model excited by an unit vertical force at Position 1: (a) vertical velocity response at Position 1; (b) vertical velocity response at Position 2; (c) the source level of the radiated sound power.

the typical stiffened cylindrical shell structure in the medium frequency region. It also shows that the results calculated by the three methods are overlapping one with another from low to high frequency regions with good concatenation.

5. EXPERIMENTAL VERIFICATION

The underwater vibration test of a ring-stiffened cylindrical shell with three substructures including a bulkhead with a piece of floor (Substructure 1), a bulkhead (Substructure 2) and a side foundation

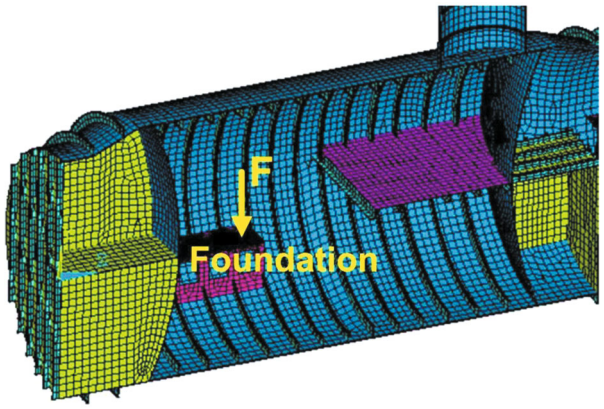

Fig. 6. Structure model of the ring-stiffened cylindrical shell structure with the foundation type substructure.

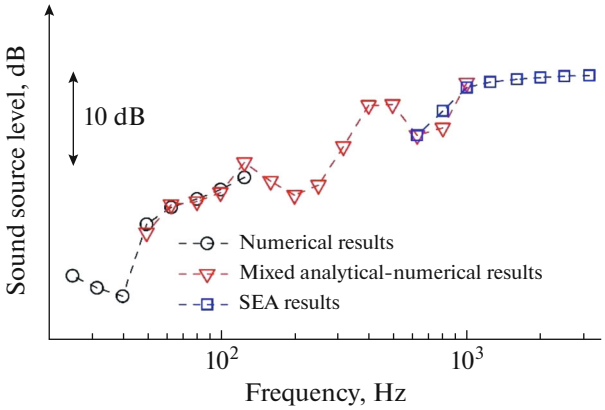

Fig. 7. The results of 1/3-oct sound source spectrum level predicted by the three methods.

(Substructure 3) as shown in Fig. 8 was carried out. An electromagnetic exciter was used to generate the vertical exciting force at the side foundation panel. The vertical acceleration at the exciting point was measured. The transfer function of the acceleration and the exciting force at the foundation panel are calculated by both the present MANS method and the numerical sono-elastic analysis method in different frequency regions. The calculated results are compared with the test results in Fig. 9. The truncated axial and circumferential mode orders used in the MANS method are $M = 44$ and $N = 22$.

It shows that in general the prediction of the numerical sono-elastic analysis method in low frequency region and the prediction of the MANS method in the medium frequency region agree with the test results fairly good. At the frequency region above 200 Hz there appear some differences. Some of the reasons may be that the calculation model does not precisely reflect the test model, such that the test

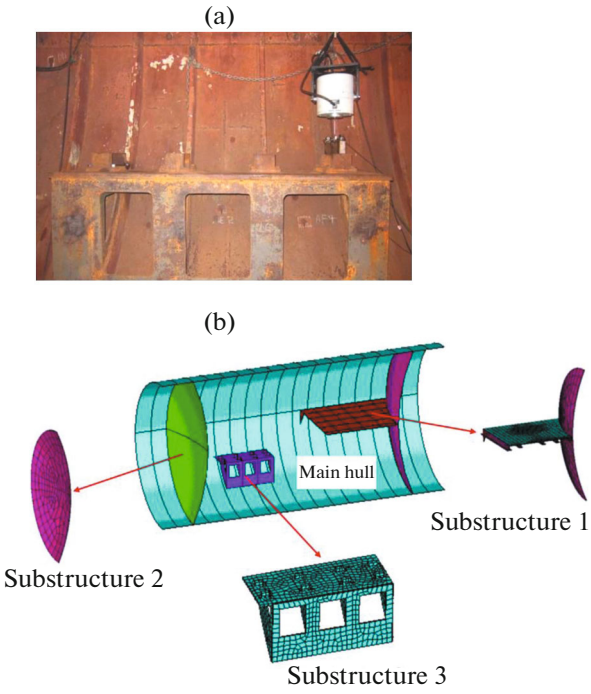

Fig. 8. The model used for experimental verification: (a) the vibration test; (b) the calculation model.

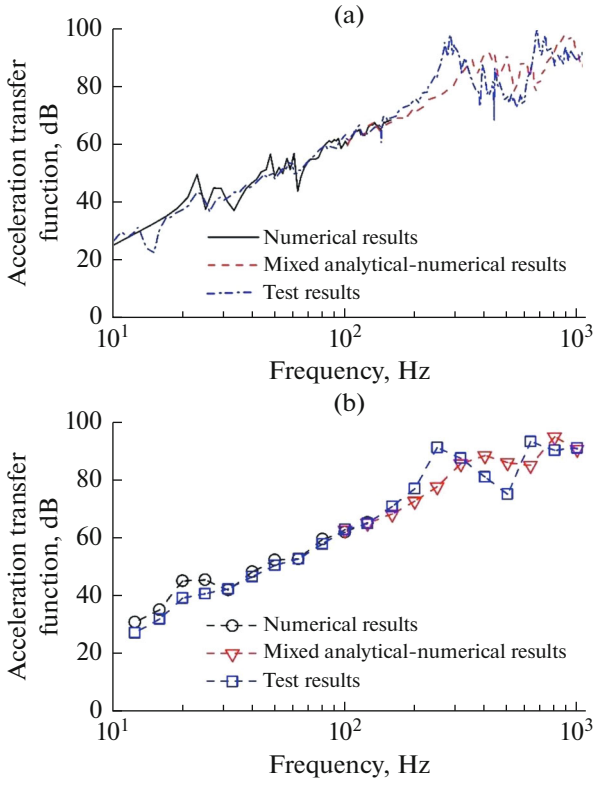

Fig. 9. Comparison of predictions and test results of acceleration transfer functions (ref 1×10^{-6} m/s^2) excited and measured at the foundation panel: (a) spectrum density level; (b) 1/3-oct spectrum level.

model was only a cabin of the cylindrical vehicle, its two ends were not simply supported, neither attached with long rigid barrier pillars, as was assumed in the analytical solutions of the MANS method; the two end plates of the test model are interacting with fluid leading to increased hydrodynamic added mass, etc.

The MANS method presented in this work is proposed considering both the computational cost and the precision. The purely numerical model of a real scale ship structure is much more suitable for the vibro-acoustic analysis in the frequency range below 200 Hz. In the frequency range above 700 Hz, the Statistical Energy Analysis (SEA) method is a better choice. The MANS method is mainly used in the frequency band from 200 to 700 Hz. Therefore, Figs. 7 and 9 proved that the MANS method can play a role of connecting the frequency range below 200 Hz and the frequency band above 700 Hz.

6. CONCLUSIONS

The Mixed Analytical-Numerical Substructure (MANS) method is proposed in this paper to predict vibrations and acoustic radiations of cylindrical-shell-type underwater ship structures in medium frequency region. In this method, the interactions of the structure and the acoustic medium of the main hull are dealt with by analytical method for increasing the frequency range and the calculation efficiency. The effect of local substructures is modeled by the FEM and incorporated into the analysis by the super-element method of modal synthesis [20]. The purpose of proposing this method is to make the prediction of the vibration and acoustic radiation behaviors of the modified or optimized substructures more efficient and convenient. The calculation frequency range may also be extended higher than the three-dimensional numerical sono-elastic analysis method [18], and hence is suitable in the medium frequency region, in compensation with the three-dimensional numerical sono-elastic analysis method for low frequency region and the SEA method for high frequency region.

The applicability and the accuracy of the MANS method and the corresponding code are validated by comparisons in two numerical examples with the above mentioned two other methods, and the comparison with the results of a model test. It proves that the MANS method is suitable for prediction of vibrations and acoustic radiations of typical cylindrical-shell-type submerged structures in the medium frequency region.

ACKNOWLEDGMENTS

This work was supported by the National Key R&D Program of China (Grant no. 2017YFB0202701), the

National Natural Science Foundation of China (Grant nos. 11772304, 51709241), and the Natural Science Foundation of Jiangsu Province of China (Grant no. BK20170216).

REFERENCES

1. W. L. Wang and Z. R. Du, *Structure Vibration and Dynamic Substructure Analysis Method* (Fudan Univ. Press, Shanghai, 1985).
2. X. G. Yin, H. Chen, and K. L. Jian, *Substructure Method for Structure Vibration Analysis* (China Railway Publ. House, Beijing, 1991).
3. M. Amabili, J. Fluids Struct. **11** (5), 507 (1997).
4. C. P. Zou and D. S. Chen, J. Shanghai Jiaotong Univ. **37**, 1213 (2003).
5. P. Persson, K. Persson, and G. Sandberg, J. Fluids Struct. **61**, 205 (2016).
6. B. Laulagnet and J. L. Guyader, J. Sound Vib. **138**, 173 (1990).
7. C. Soize, J. Acoust. Soc. Am. **94**, 849 (1993).
8. L. P. Franzoni and C. D. Park, J. Acoust. Soc. Am. **108**, 2856 (2000).
9. C. D. Park, J. Acoust. Soc. Am. **116**, 2956 (2004).
10. J. Liang and B. A. T. Petersson, J. Sound Vib. **247**, 703 (2001).
11. A. Pratellesi, M. Viktorovitch, N. Baldanzini, and M. Pierini, J. Sound Vib. **309**, 545 (2008).
12. V. Meyer, L. Maxit, J. L. Guyader, and T. Leissing, J. Sound Vib. **360**, 260 (2016).
13. V. Meyer, L. Maxit, and C. Audoly, J. Acoust. Soc. Am. **140**, 1609 (2016).
14. M. B. Salin, E. M. Sokov, and A. S. Suvorov, Hydroacoustics **14**, 36 (2011
15. A. S. Suvorov, E. M. Sokov, and P. V. Artel'nyi, Acoust. Phys. **60**, 694 (2014).
16. M. S. Zou and Y. S. Wu, J. Ship Mech. **18**, 574 (2014).
17. M. S. Zou, PhD Thesis (China Ship Scientific Research Center, Wuxi, 2014).
18. M. S. Zhou, Y. S. Wu, and Y. L. Ye, J. Hydrodyn., Ser. B **22**, 844 (2010).
19. R. E. D. Bishop, W. G. Price, and Y. S. Wu, Philos. Trans. R. Soc. London, Ser. A **316**, 375 (1986).
20. W. J. Yun, G. B. Duan, and Z. G. Hu, Shanghai Mech. **4**, 8 (1982).
21. D. Ranlet, F. L. Dimaggio, H. H. Bleich, and M. L. Baron, Comput. Struct. **7**, 355 (1977).
22. Z. Y. Cao, *Vibration Theory of Plates and Shells* (China Railway Publ. House, Beijing, 1989).
23. P. R. Stepanishen, J. Acoust. Soc. Am. **71**, 813 (1982).
24. S. X. Liu and M. S. Zou, J. Acoust. Soc. Am. **143**, EL160 (2018).
25. F. B. Jensen, W. A. Kuperman, M. B. Porter, and H. Schmidt, *Computational Ocean Acoustics*, 2nd ed. (Springer, New York, 2011).
26. M. S. Zou, Y. S. Wu, and Y. M. Liu, Acta Mech. Sin. **30**, 59 (2014).